Cell Transplantation, Vol. 18, pp. 283–295, 2009
Printed in the USA.

0963-6897/09 $90.00 + .00
E-ISSN 1555-3892
www.cognizantcommunication.com

Implantation of a Three-Dimensional Fibroblast Matrix Improves Left Ventricular Function and Blood Flow After Acute Myocardial Infarction

Hoang M. Thai,* Elizabeth Juneman,* Jordan Lancaster,* Tracy Hagerty,* Rose Do,* Lisa Castellano,* Robert Kellar,† Stuart Williams,‡ Gulshan Sethi,* Monika Schmelz,* Mohamed Gaballa,*§ and Steven Goldman*

*Section of Cardiology, Department of Medicine and Pathology, Southern Arizona VA Health Care System, Sarver Heart Center, University of Arizona, Tucson, AZ, USA
†Northern Arizona University, Flagstaff, AZ, USA
‡Jewish Hospital, Louisville, KY, USA
§Theregen Inc., San Francisco, CA, USA

This study was designed to determine if a viable biodegradable three-dimensional fibroblast construct (3DFC) patch implanted on the left ventricle after myocardial infarction (MI) improves left ventricular (LV) function and blood flow. We ligated the left coronary artery of adult male Sprague-Dawley rats and implanted the 3DFC at the time of the infarct. Three weeks after MI, the 3DFC improved LV systolic function by increasing ($p < 0.05$) ejection fraction ($37 \pm 3\%$ to $62 \pm 5\%$), increasing regional systolic displacement of the infarcted wall (0.04 ± 0.02 to 0.11 ± 0.03 cm), and shifting the passive LV diastolic pressure volume relationship toward the pressure axis. The 3FDC improved LV remodeling by decreasing ($p < 0.05$) LV end-systolic and end-diastolic diameters with no change in LV systolic pressure. The 3DFC did not change LV end-diastolic pressure (LV EDP; 25 ± 2 vs. 23 ± 2 mmHg) but the addition of captopril (2mg/L drinking water) lowered ($p < 0.05$) LV EDP to 12.9 ± 2.5 mmHg and shifted the pressure–volume relationship toward the pressure axis and decreased ($p < 0.05$) the LV operating end-diastolic volume from 0.49 ± 0.02 to 0.34 ± 0.03 ml. The 3DFC increased myocardial blood flow to the infarcted anterior wall after MI over threefold ($p < 0.05$). This biodegradable 3DFC patch improves LV function and myocardial blood flow 3 weeks after MI. This is a potentially new approach to cell-based therapy for heart failure after MI.

Key words: Acute myocardial infarct; Fibroblasts; Growth factors; Angiogenesis; Extracellular matrix; Bioabsorbable scaffold

INTRODUCTION

Cell-based therapy with direct injection of cells into the infarcted heart is currently being examined as a new treatment for heart failure. While a number of different cell types have been shown to improve left ventricular (LV) function in animal models of acute ischemic damage, the results of direct cell injection into the heart in clinical trials has been less dramatic (1,3,13,19,28–32, 36). In part, this appears to be because few of the transplanted cells survive when injected into the infarcted heart (2,14,21,34). While the explanation for this is not clear, it may be that injecting cells directly into injured myocardium or scar tissue is a problem because this damaged tissue is not a supportive milieu (i.e., scar tissue has an inadequate blood supply with insufficient viable tissue or matrix support for new cells to attach, survive, and grow).

Because of these drawbacks, we have developed a different approach to cell-based therapy for heart failure; we implant a matrix graft onto the infarcted heart to provide a support structure for new blood vessel growth (10). This matrix provides a more hospitable environment for cell migration and growth into the damaged left ventricle. In this report we provide data on a three-dimensional biodegradable dermal fibroblast construct (3DFC) that is a matrix-embedded human construct of newborn dermal fibroblasts cultured in vitro onto a bioabsorbable mesh to produce a living, metabolically active tissue that has the potential to increase new blood vessel formation in vivo (15,16).

Our hypothesis is that the 3DFC matrix or patch graft will improve LV function and increase myocardial blood flow when implanted onto an infarcted heart. To test this hypothesis, we created an anterior wall myocardial infarction (MI) by ligating the left coronary artery of

Address correspondence to Steven Goldman, M.D., Cardiology Section, 1-111C, Southern Arizona VA Health Care System, 3601 S. 6th Avenue, Tucson, AZ 85723, USA. Tel: (520) 792-1450, ext. 5081; Fax: (520) 629-4636; E-mail: steven.goldman@va.gov

rats, implanted the 3DFC patch at the time of surgery and used solid-state micrormanometers to measure hemodynamics, two-dimensional echocardiography to measure LV regional wall motion, function, chamber size, immunohistochemistry for microvessel density analysis, and neutron-activated microspheres to measure myocardial blood flow. We treated a separate group of infarcted rats with a combination of the 3DFC patch and captopril in order to simulate the clinically relevant situation where a patient in heart failure after a MI is treated with an angiotensin converting enzyme inhibitor. The data show that the 3DFC patch improves blood flow, regional wall motion in the infarcted left ventricle, ejection fraction (EF), and partially reverses maladaptive LV remodeling after MI. We do not see these results when a nonviable patch alone is placed over the infarcted myocardium. The addition of captopril to the 3DFC also lowers LV end-diastolic pressure (LV EDP) and shifts the LV pressure–volume relationship toward the pressure axis. This study shows that placing a viable fibroblast matrix on the infarcted myocardium may be a new approach to cell-based therapy for heart failure after a MI.

MATERIALS AND METHODS

Study Design and Treatment Groups

To test the efficacy of the 3DFC in the treatment of heart failure after MI, we had five treatment groups: sham ($N = 14$); MI ($N = 18$); MI + 3DFC ($N = 11$); MI + 3DFC (nonviable) ($N = 12$); MI + 3DFC + captopril ($N = 8$).

Coronary Artery Ligation Experimental MI

Heart failure is created in rats using standard techniques in our laboratory (8,9,12,24,26,33). In brief, rats are anesthetized with ketamine and acepromazine and a left thoracotomy performed. The heart is expressed from the thorax and a ligature placed around the proximal left coronary artery. The heart is returned to the chest and the thorax closed. The rats are maintained on standard rat chow, water ad libitum, and pain medication postoperatively. The experimental protocols are approved by the animal use committees of the Southern Arizona VA Health Care System and the University of Arizona, guaranteeing that all animals have received human care in compliance with the Guide for the Care and Use of Laboratory Animals (www.nap.edu/catalog/5140.html). Infarcted rats undergoing this procedure have large MIs averaging 40% of the ventricle (8,12). Myocardial infarction is confirmed by hemodynamics (LV end-diastolic pressure >16 mmHg) and presence of a scar. Prior to closing the chest, the 3DFC patch is engrafted onto the injured myocardium with the chest open as described below. The lungs are inflated, the chest closed, and the rat allowed to recover. We treated two other separate groups of rats: MI and captopril (2 g/L drinking water) and MI + 3DFC patch and captopril (2 g/L drinking water) for 3 weeks.

The 3DFC Patch

The 3DFC patch is a cryopreserved human fibroblast-derived tissue composed of fibroblasts, extracellular matrix, and a bioabsorbable scaffold (15,16). Figure 1 is a scanning electron micrograph of the 3DFC showing that the vicryl fibers are "tube-like" structures. The fibroblasts look like irregular structures with long appendages that span from one vicryl fiber to another. The fibroblast cells are from a qualified cell bank, which has been extensively tested for animal viruses, retroviruses, cell morphology, karology, isoenzymes, and tumorgenicity. Reagents used in the manufacture of the 3DFC patch are tested and found free from viruses, retroviruses, endotoxins, and myocoplasma before use. One piece of approximately 2×3 in. (5×7.5 cm) in size is supplied frozen in a clear bag for a single-use application. The patch remains frozen at -75 ± 10°C continuously until ready for use when it is placed in a sterile bowl containing PBS (34–37°C). The patch is handled gently by the edges to limit cellular damage and applied to the heart within 60 min of being removed from its container (Fig. 2). The 3DFC patch was provided by Theregen, Inc. (San Francisco, CA).

To separate the effects of the cells from physical effects of the vicryl we examined the effects of nonviable 3DFC. The nonviable 3DFC is the standard 3DFC that is rendered nonviable by storage for 9 or more days at –20°C. The nonviable 3DFC consists of the same biodegradable vicryl mesh with fibroblasts and extracellular matrix with matrix-bound growth factors and cytokines. The fibroblasts are killed with the higher temperature freeze phase (–20°C), leaving behind the standard extracellular matrix (tissue) and matrix-bound proteins as well as the cellular debris. However, the nonviable 3DFC no longer contains viable, living cells.

The viable 3DFC does not generate an immune response. Developmental work on 3DFC includes experiments in dogs treated with 3DFC showing no immune response (Investigators' brochure ITT-101, Theregen). The work reported here is the first in an immune-competent animal showing that the benefits of the 3DFC are not related to the immune status of the recipient. The low immunoginecity of allogeneic fibroblasts grown on a scaffold is thought to be due to the fact that the majority of these fibroblasts show little induction of CD40 and HLA-DR in response to γ-interferon (17). The 3DFC patch is FDA approved for wound healing; it has been used in over 20,000 patients mostly as a skin graft for diabetic foot ulcers with no untoward complications. There is no activation of the immune system in patients

Figure 1. Scanning electron micrograph of the 3DFC patch. The vicryl fibers are "tube-like" structures. The fibroblasts look like irregular structures with long appendages that span from one vicryl fiber to another.

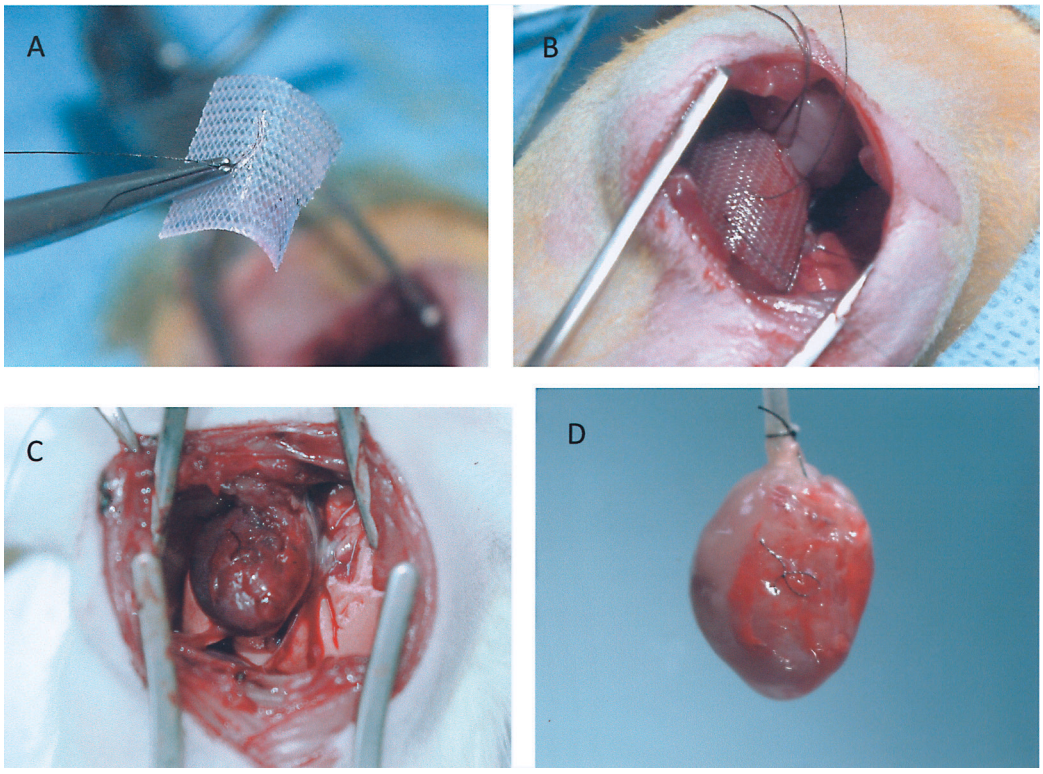

Figure 2. (A) Three-dimensional fibroblast culture (3DFC) prior to implantation; the suture in the middle of the patch is used to attach the 3DFC to the left ventricle. (B) 3DFC at the time of implantation on the infarcted left ventricle. (C) 3DFC at 3 weeks after myocardial infarction. Note that the 3DFC is well integrated and attached to the infarcted wall. (D) 3DFC in a perfused heart preparation at 3 weeks after myocardial infarction. As note above, the 3DFC is well integrated into the infarcted wall and the suture is easily visible.

treated with this patch for diabetic foot ulcers, other skin repair, and oropharyngeal palate repair.

Hemodynamic Measurements

We measure hemodynamics using methods reported previously by our laboratory (9,10,24–26,33). In brief, rats are anesthetized with inactin (100 mg/kg IP injection) and placed on a specially equipped operating table with a heating pad to maintain constant body temperature. Following endotracheal intubation and placement on a rodent ventilator, a 2F solid state micromanometer tipped catheter with two pressure sensors (Millar) is inserted via the right femoral artery, with one sensor located in the left ventricle and another in the ascending aorta. The pressure sensor is equilibrated in 37°C saline prior to obtaining baseline pressure measurements. After a period of stabilization, LV and aortic pressures, and heart rate are recorded and digitized at a rate of 1000 Hz using a PC equipped with an analog-digital converter and customized software. From these data, LV dP/dt is calculated.

LV Pressure–Volume Relationships

The LV pressure–volume relationship is measured as outlined in our previous work (8,12). In brief, the heart is arrested with potassium chloride, and a catheter consisting of PE-90 tubing with telescoped PE-10 tubing inside is inserted into the LV via the aortic root. One end of the double-lumen LV catheter is connected to a volume infusion pump (Harvard Apparatus) while the other end is connected to a pressure transducer zeroed at the level of the heart. The right ventricle is partially incised to prevent loading on the LV. The LV is filled (1.0 ml/min) to 60–100 mmHg and unfilled while pressure is recorded onto a physiologic recorder (Gould). Ischemic time is limited to 10 min. Volume infused is a function of filling rate.

Echocardiography

We perform closed chest transthoracic echocardiography at baseline prior to the MI, immediately after MI, and at 3 weeks after MI using methods previously developed in our laboratory (33). We use a Vingmed, Vivid 7 system echo machine (GE Ultrasound) with EchoPac (GE Ultrasound) programming software with a 10 MHz multiplane transducer with views in the parasternal short axis and long axis, to specifically evaluate the anterior, lateral, anterolateral, inferior, and posterior walls. Two-dimensional (2D) and M-mode measurements of myocardial wall thickness and LV dimensions are obtained throughout the cardiac cycle and are used for calculation of systolic displacement of the anterior wall, ejection fraction, and regional fractional shortening. Systolic displacement is a measure of focal LV wall thickening. Using M-mode through the anterior wall of the left ventricle, the LV wall thickness is measured at diastole and systole; the difference in the thickness between the two measurements is the systolic displacement. This is a useful measurement to quantify focal LV wall systolic function.

Myocardial Perfusion

We use neutron activated microspheres (BioPal Inc, Worcester MA) to measure myocardial blood flow. The isotopes are injected, a tissue sample obtained, and at a later time activated with the emitted radiation measured with high-resolution detection equipment (7,18,27). With this system, BioPal, Inc. provides the isotopes and tissue containers. Three separate isotopes (lutetium, gold, and samarium) are injected in each rat: one at baseline prior to coronary ligation, one immediately after ligation, and one at the endpoint of the study. Because different rats are used for each group we are able to obtain end point data after different treatments (MI at 3 weeks, MI at 3 weeks + 3DFC). For each measurement 750,000 nonradioactive elementally labeled 15-μm microspheres (V = 300 μl) from Biopal, Inc. are injected into the left ventricle transapically with a 1-cc syringe and 27-gauge needle. At the terminal study point, the tissues are harvested, oven dried, and collected for analysis. At the time of microsphere injection we perform a transthoracic echocardiogram to measure stroke volume. By knowing the heart rate, we calculate cardiac output as stroke volume × heart rate. Assuming 4% of the cardiac output perfuses the coronary arteries (27), we know the total myocardial blood flow; the number of microspheres deposited in the anterior wall is percentage of blood flow down the left coronary artery to the anterior wall at each time point.

Histopathology

Hearts were formalin fixed (10%) prior to paraffin embedding. HIER antigen retrieval of 3-μm-thick sections was performed in citrate-based Diva buffer (pH 6.2) for 1 min at 125°C using a "Decloaker" pressure cooker (Biocare Medical Concord, CA). We used single immunohistochemical staining for anti-rabbit factor VIII (Dako) (1:1000) to perform histological analysis of microvessel density.

Vessel Density

We defined vessel density by light microscopy at 40× magnification. The number of cross section vessels per field was counted by two persons blinded to treatment. Average measurements from six different fields were recorded for each value. Knowing the area of the optical field, data are reported as number of vessels/μm^2.

Statistical Analysis

Data are expressed as mean ± SE. For the physiologic and echocardiographic measurements, the effects of the 3DFC were determined by using two-way analysis of variance followed by the Student *t*-test. The value of $p < 0.05$ was accepted as significant. The authors had full access to the data and take responsibility for its integrity. All authors have read and agree to the manuscript as written.

RESULTS

In Vivo Hemodynamics

Rats with MI had a fourfold increase in left ventricular end diastolic pressure, a 22% reduction in LV systolic blood pressure, a 24% reduction in mean arterial blood pressure, a 37% reduction in left ventricular dP/dt, and a 21% prolongation of the time constant of LV relaxation or tau (Table 1). The baseline data are consistent with our previous reports using this model showing that ligation of the left coronary artery results in a large anterior wall MI and heart failure with a decrease in LV systolic function, an elevation of LV EDP, and a prolongation of tau (8,9,12,24–26,33). The 3DFC lowered ($p < 0.05$) mean arterial pressure and increased ($p < 0.05$) peak developed pressure or PDP (126 ± 4 to 146 ± 8 mmHg).

Captopril Treatment

Treatment with captopril after MI lowered ($p < 0.05$) MAP, LV SP, and LV EDP; these changes are similar to what we and other investigators have previously shown (26). The addition of captopril in the 3DFC rats lowered LV EDP from 23 ± 2 to 13 ± 3 mmHg and PDP from 146 ± 8 to 123 ± 5 mmHg ($p < 0.05$); all other hemodynamic parameters were unchanged (Table 1). Vascular resistance increased ($p < 0.05$) with acute MI from 2.3 ± 3.7 to 9.1 ± 1.9 mmHg/ml/min; compared to acute MI, vascular resistance in chronic heart failure was unchanged at 7.7 ± 0.92 mmHg/ml/min. The 3DFC decreased ($p < 0.05$) vascular resistance to 3.9 ± 0.86; the addition of captopril further decreased ($p < 0.05$) vascular resistance to 0.41 ± 0.03 mmHg/ml/min.

Echocardiographic Changes in LV Function and PV Loops

The data on global and regional changes in LV function are seen in Figures 3, 4, 5, and 6. There was a decrease ($p < 0.05$) in LV EF (75 ± 4% to 37 ± 3%) with the acute MI and a subsequent increase ($p < 0.05$) with the 3DFC patch (53 ± 4%). The EF did not increase with the nonviable 3DFC (31 ± 2%); the addition of captopril to the 3DFC did not change the EF compared to 3DFC alone (48 ± 3%). The changes in regional LV function, defined as systolic displacement calculated from parasternal short axis M-mode echocardiography, were similar. With the coronary ligation, there was a decrease ($p < 0.05$) in systolic displacement of the anterior infarcted wall (0.15 ± 0.03 to 0.05 ± 0.02 cm) with a return toward normal with the placement of the 3DFC patch (0.11 ± 0.04 cm). The nonviable 3DFC did not alter EF or systolic displacement.

The LV end-diastolic diameter increased ($p < 0.05$) from 4.6 ± 0.4 to 8.1 ± 0.3 mm and the LV end-systolic diameter increased ($p < 0.05$) from 1.2 ± 0.2 to 4.1 ± 0.7 mm 3 weeks after MI (Fig. 5). The 3FDC patch decreased ($p < 0.05$) LV end-diastolic diameter to 6.6 ± 0.4 mm and end-systolic diameter to 1.8 ± 0.08 mm. The PV relationship shows dilatation of the ventricle with the MI but no shift when the 3DFC patch was added (Fig. 6). The addition of captopril to the 3DFC shifted the PV loop to the left toward the pressure axis and deceased the operating LV end-diastolic volume from 0.57 ±

Table 1. Hemodynamics for 3DFC Patch/Captopril After MI

	MAP (mmHg)	HR (bpm)	LV SP (mmHg)	LVEDP (mmHg)	LV dP/dt (mmHg/s)	PDP (mmHg)	Tau (ms)
Sham ($N = 14$)	106 ± 5	287 ± 15	124 ± 5	7 ± 1	7360 ± 379	192 ± 18	19.0 ± 1.3
MI ($N = 18$)	90 ± 2*	269 ± 13	103 ± 3*	25 ± 2*	4542 ± 215*	126 ± 4	24.2 ± 1.8*
MI + captopril ($N = 11$)	72 ± 3*	283 ± 15	88 ± 3†‡	14 ± 2†	4398 ± 315*	118 ± 7*	21.8 ± 1.8*
MI + 3DFC (viable) ($N = 11$)	84 ± 3†	248 ± 10	100 ± 5*	23 ± 2*‡	4242 ± 156*	146 ± 8†§	29.7 ± 3.5*
MI + 3DFC (nonviable) ($N = 12$)	88 ± 4*	270 ± 7	102 ± 4*	24 ± 2*	4502 ± 179*	118 ± 4	26.0 ± 3.0*
MI + 3DFC (viable) + captopril ($N = 8$)	83 ± 4†	265 ± 23	100 ± 6*	13 ± 3†	4502 ± 179*	123 ± 5§	25.8 ± 2.8*

Values are mean ± SE. MAP, mean arterial pressure; MI, myocardial infarction; LV, left ventricular; LV EDP, LV end-diastolic pressure; PDP, peak developed pressure; Tau, time constant of LV relaxation; 2DFC, three-dimensional fibroblast construct.
*$p < 0.05$ versus sham.
†$p < 0.05$ versus sham and MI.
‡$p < 0.05$ versus MI + 3DFC/captopril.
§$p < 0.05$ versus sham and MI + 3DFC.

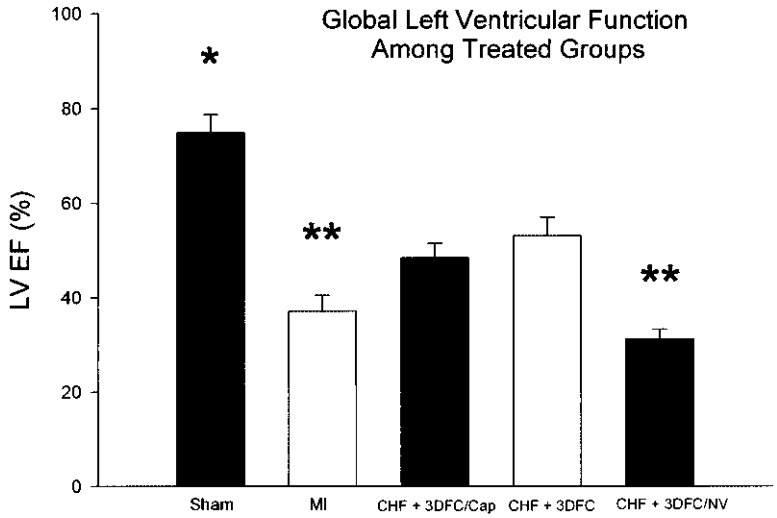

Figure 3. Echocardiographic measured ejection fraction (EF) in sham, myocardial infarction (MI), MI + 3DFC, MI + 3DFC/Cap (captopril), and MI + 3DFC/NV (nonviable). Note that the viable 3DFC increased the EF. The EF remained increased with the addition of captopril to the viable 3DFC; the nonviable 3DFC did not improve EF. Values are mean ± SE. Sham ($N = 5$); MI ($N = 8$); MI + 3DFC/cap ($N = 10$); MI + 3DFC ($N = 14$); MI + 3DFC (nonviable) ($N = 5$). *$p < 0.05$ sham versus all groups; **$p < 0.05$ MI and MI + 3DFC/NV versus MI + 3DFC/cap and MI + 3DFC.

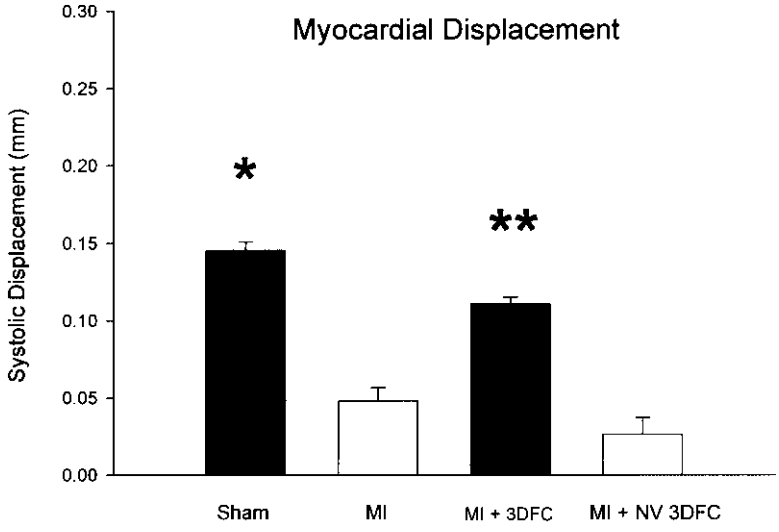

Figure 4. Echocardiographic measured systolic displacement of the infarcted anterior wall in sham, myocardial infarction (MI), and MI + 3DFC. Note that the 3DFC improved EF back toward the normal value. Values are mean ± SE. Sham ($N = 6$); MI ($N = 12$); MI + 3DFC ($N = 15$); MI + NV 3DFC ($N = 12$). *$p < 0.05$ versus MI; **$p < 0.05$ versus MI.

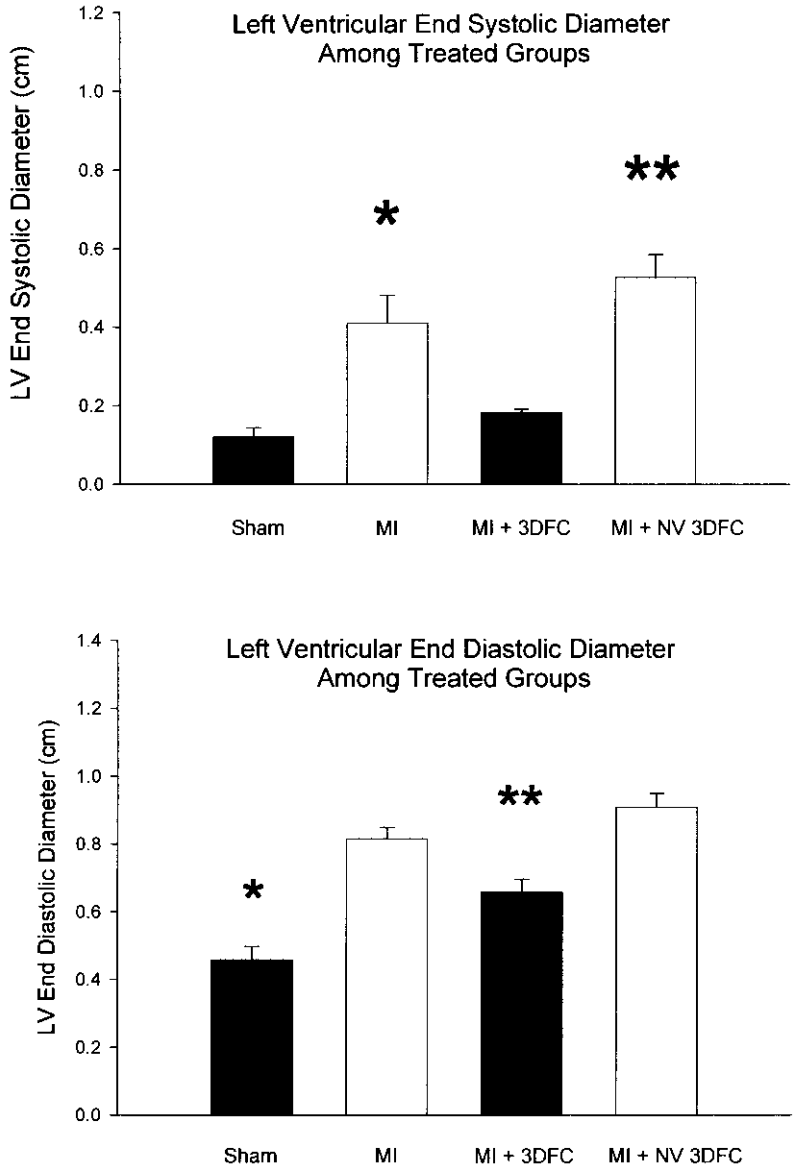

Figure 5. Echocardiographic measured LV end-diastolic and end-systolic diameters in sham, myocardial infarction (MI), and MI + 3DFC. Note that both the LV end-diastolic diameter and end-systolic diameters decrease with the 3 DFC. Values are mean ± SE. Sham (N=6); MI (N=12); MI + 3DFC (N=15); MI + NV 3DFC, (N=12). *$p < 0.05$ versus sham; **$p < 0.05$ versus MI.

0.05 to 0.34 ± 0.03 ml ($p < 0.05$). The nonviable 3DFC did not alter end-diastolic or end-systolic diameter.

Increased Blood Vessels and Myocardial Blood Flow

With acute MI, there was an approximately 80% decrease in blood flow to the infarcted wall, which was not altered at 3 weeks. With the 3DFC, the blood flow increased to about 70% of baseline (Fig. 7). The increase in blood flow was a result of new blood vessel formation with the 3DFC (Figs. 8 and 9).

DISCUSSION

The important findings in this study are that this three-dimensional biodegradable fibroblast patch increases myocardial blood flow in the damaged region of the LV and increases systolic displacement in the anterior infarcted wall after an acute MI. The 3DFC reverses maladaptive LV remodeling, by increasing EF and decreasing LV end-diastolic and end-systolic diameters. The addition of captopril lowers LV end-diastolic pres-

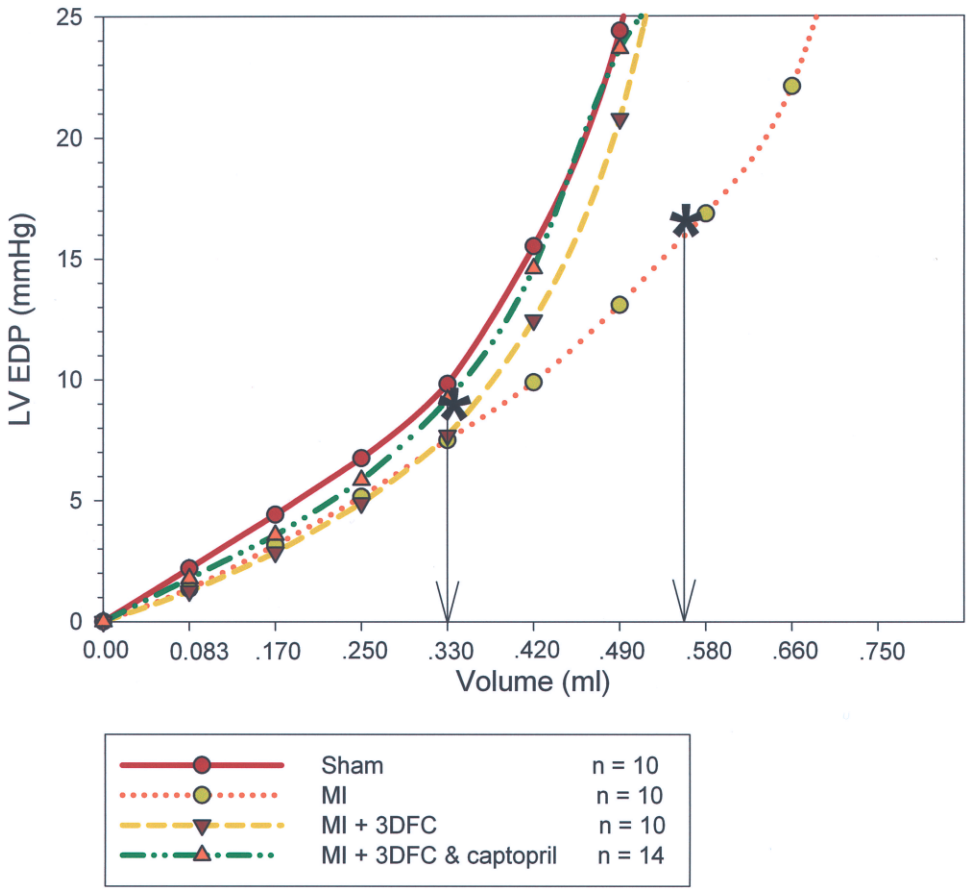

Figure 6. Pressure–volume (PV) loops in sham, myocardial infarction (MI), MI + 3DFC, and MI + 3DFC/captopril. Note that the major shift in the PV loop was with the addition of captopril where the operating LV end-diastolic volume decreased.

sures and decreases the operating LV end-diastolic volume. These data support our hypothesis that this viable fibroblast patch provides a supporting structure for the damaged heart and may be an alternative to direct cell injection for cell-based therapy for heart failure after MI.

Cell-Based Therapy for Heart Failure

While the original animal data with cell-based therapy for heart failure were very encouraging, the results from the most recent clinical trials with direct cell injection into the heart and/or coronary arteries have been disappointing. Clinical trials such as the BOOST, TOPCARE, the IACT, the REPAIR-MI, the ASTAMI Trial, and a bone marrow transplant study from Belgium of intracoronary delivery of autologous bone marrow cells in patients after MI with PCI show only modest improvement in LV function, mostly in patients with preserved EFs with some questions about delivery techniques (1,3,13,19,23,28–32,36). The most positive results are a subset analysis of the REPAIR-MI trial showing that at 1 year, bone marrow cell injection with a higher percentage of $CD34^+$ cells decreases reinfarctions and revascularization procedures with revascularizations driving an improved composite end-point of revascularizations, MI, and death (30). We believe that this general lack of positive results with direct cell injection is due in part to the observation that most of these newly injected cells do not survive chronically in the infarcted heart and do not transdifferentiate into cardiac myocytes (2,21,34). Investigators are now injecting cardiac stem cells into the heart in an attempt to obviate the need for stem cells to transdifferentiate (23).

Three-Dimensional Fibroblast Patch

Our hypothesis is that the lack of survival of new cells directly injected into the heart is related, in part, to an inadequate blood supply and inadequate matrix support for the new cells. The injected cells are fragile, resulting in cell aggregation due to lack of physical support for the cells to attach to the tissue extracellular

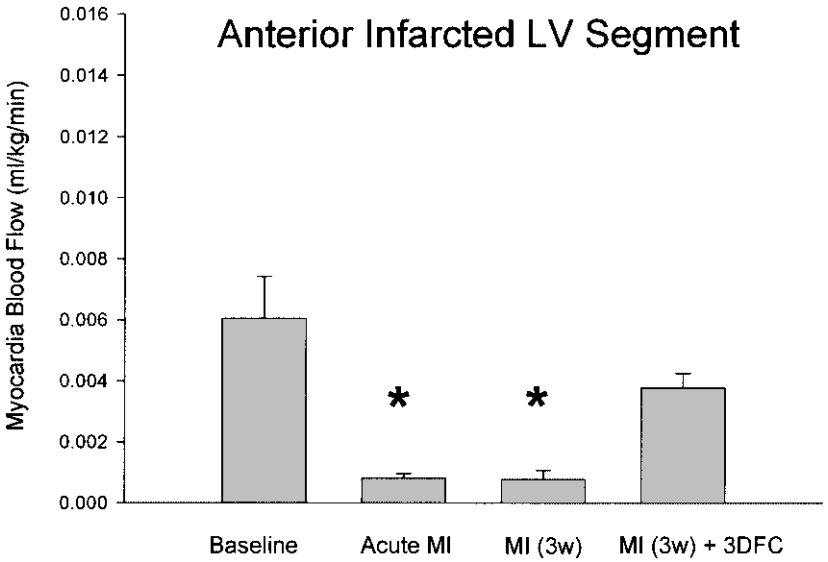

Figure 7. Anterior wall myocardial blood flow in sham ($N = 11$), at the time of acute myocardial infarction (MI, $N = 7$), MI at 3 weeks ($N = 4$), and MI at 3 weeks with 3DFC ($N = 4$). Note that the 3DFC improved blood flow in the infarcted wall. Values are mean ± SE; $*p < 0.05$ versus baseline and MI (3w) + 3DFC.

matrix. This three-dimensional scaffold offers a potential solution to the problem of an inadequate support structure. While injection of passive materials has been proposed to improve EF potentially by decreasing wall stress (11,35), the 3DFC provides a viable cell matrix that supports new blood vessel growth (15,16). This viable cellular matrix is important because in addition to providing a new support structure for the damaged heart, we also need to create a mature blood supply such that new viable cardiac muscle can be organized in parallel forming physical and neural connections that will conduct electrical signals and create synchronized contractions. Investigators have proposed that the ideal scaffold structure for the heart would consist mainly of highly

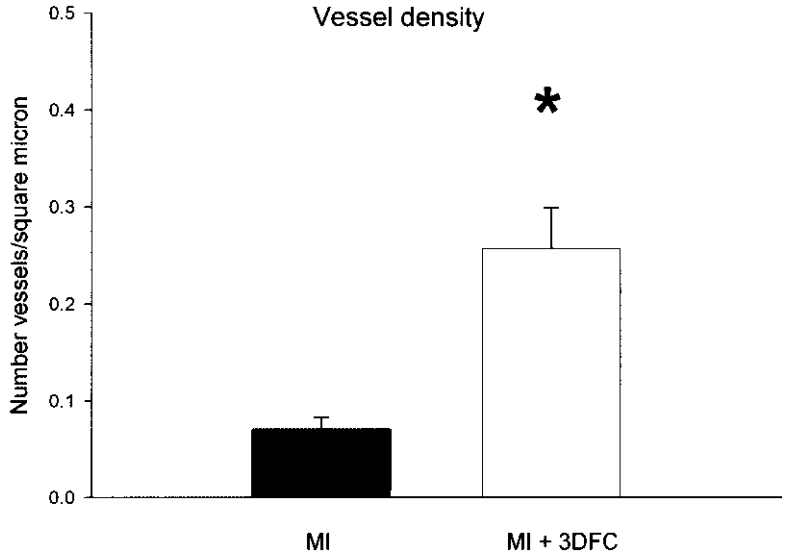

Figure 8 Vessel density defined by Factor VIII staining. Note the increase in vessel density in the area with the 3DFC compared to the untreated myocardial infarction (MI). MI ($N = 9$), MI + 3DFC ($N = 8$). Values are mean ± SE. $*p < 0.05$ versus MI.

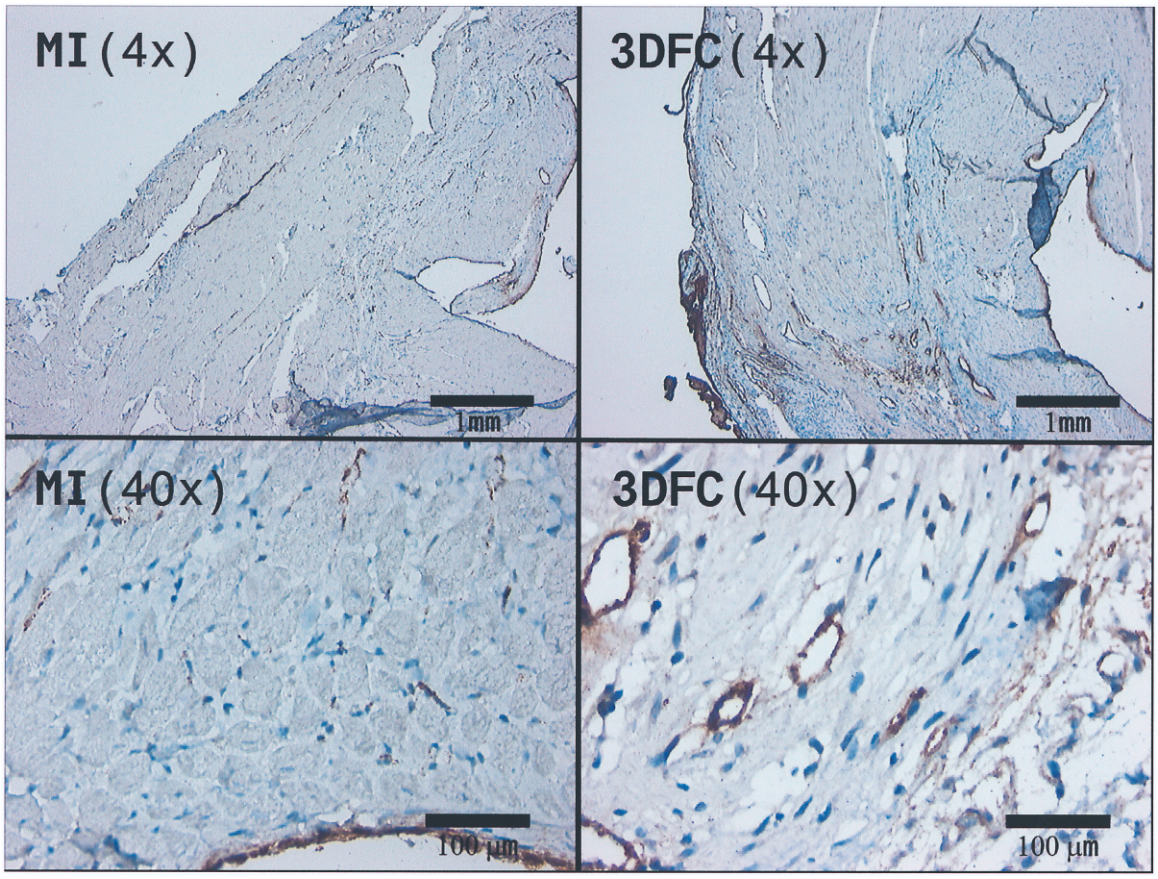

Figure 9. Histopathology sections of Factor VIII staining in MI + 3DFC (A–C) and MI alone (4× and 40×). Note the increased in Factor VIII staining and vessel density with the 3DFC.

interconnected pores with a diameter of at least 200 µm, the average size of a capillary, to permit blood vessel penetration and cell interactions (5).

The 3DFC is a viable construct composed of a matrix embedded with human newborn dermal fibroblasts cultured in vitro onto a bioabsorbable mesh to produce living, metabolically active tissue (15,16) (see Figs. 1 and 2). As the fibroblasts proliferate across the mesh, they secrete human dermal collagen, fibronectin, and glycosaminoglycans (GAGs), embedding themselves in a self-produced dermal matrix. The fibroblast cells produce angiogenic growth factors: vascular endothelial growth factor (VEGF), hepatocyte growth factor (HGF), basic fibroblast growth factor (bFGF), and angiopoietin-1. The construct is grown in medium supplemented with serum and ascorbate; at harvest, the medium is replaced with a 10% DMSO-based cryoprotectant, the tissue is frozen and stored at −70°C. This cryopreservation and rewarming technique has been extensively studied to ensure viability of the patch. Although the mechanisms of action of the 3DFC are not completely understood, new blood vessel growth has been documented previously in SCID mice (15).

Previous work using the 3DFC as a patch for the infarcted heart in SCID mice showed histological evidence of new blood vessel growth and improvements in global LV function using a conductance catheter (16). Our data show increases in myocardial blood flow in the infarcted heart, confirming that these blood vessels are functional and that they connect to the native myocardium. We used echocardiography to document improvements in global and regional LV function. The improvements in regional LV function are important because recent work suggests that the injection of passive materials alone may be enough to reduce wall stress and increase global EF (35). In order to prove that cell-based therapy is affecting more than a passive response, the point has been made that it is necessary to be able to define regional changes in the area of the infarcted myocardium (11). We have done this using echocardiography to document that the 3DFC increases systolic displacement of the infarcted regional anterior wall (Fig. 5). Although the

mechanism of action of the 3DFC has not been completely delineated, the viable fibroblasts secrete a number of growth factors, thus providing a paracrine effect to stimulate new blood vessel growth. The vicryl mesh is biodegradable such that, with dissolution, the new blood vessel growth is in the previously damaged myocardium. The most likely explanation for the improvements in regional systolic displacement of the anterior wall is that the increases in myocardial blood flow in the border zone results in recruitment of hibernating or stunned cardiac myocytes.

The fact that the 3DFC is viable with fibroblasts implanted on a mesh is important. There are data showing that inert biodegradable patches are beneficial in treating heart failure. In our laboratory we have shown that an inert biodegradable collagen patch placed on the rat heart after a nontransmural MI improves LV function and prevents adverse LV remodeling (10). There are clinical trials with a collagen type 1 matrix seeded with autologous bone marrow cells in patients undergoing coronary artery bypass surgery (4). The best known implanted mechanical constraint device is the Acorn Corp Cap device; it decreases LV size but does not cause constrictive physiology (22). There are no blood flow studies with the Acorn device. There is a recent report using an inert biodegradable polyester urethane cardiac patch applied to rats 2 weeks after coronary ligation where the LV cavity size does not change but fractional area change increases and compliance improves; there are no blood flow data in this report (6).

Application of a Patch as an Alternative to Direct Cell Injection

The use of a biodegradable patch that provides a support structure allowing new cells to attach and grow in a damaged heart is a possible alternative to the current approach of direct cell injection for cell-based therapy. Not only are the results from current clinical trials of cell-based therapy disappointing, the approach used in these trials is cumbersome, requiring harvesting bone marrow and a repeat cardiac catheterization with infarct artery reocclusion to reinject purified autologous mononuclear cells into the coronary arteries. Another problem is the recent report that intracoronary delivery of bone marrow cells results in damage to the coronary artery with luminal loss in the infarct related artery (20). These data suggest that we need new options for cell-based therapy for heart failure.

The translational aspect of this work is important; there is potential for clinical application of this 3DFC patch. At present there are two ongoing phase I clinical trials using the 3DFC; the first is a pilot trial in patients applying the 3DFC patch at the time of coronary artery bypass surgery when the surgeon cannot place a graft to a area of viable myocardium. This trial is designed to determine if the 3DFC increases myocardial perfusion to an area that the surgeon could not graft. While in this clinical study the 3DFC patch is placed with the chest open, two cases have been done with a minimally invasive approach using a modified video-assisted thoracscopic surgery VATS procedure. The second trial is in patients getting a left ventricular assist device (LVAD). The 3DFC is applied at the time of LVAD placement and, upon LVAD removal, histology is done on the area of 3DFC placement in order to examine for evidence of angiogenesis.

Summary

We report improvements in myocardial blood flow, regional and global LV function, and partial reversal of LV remodeling using a viable three-dimensional fibroblast patch implanted in rats at the time of an acute MI. This patch provides a support structure that allows cells to grow into the damaged heart and creates new blood vessel growth, resulting in improved blood flow. With the limited success of direct cell injection into the heart, the 3DFC represents a new approach to cell-based therapy for heart failure.

ACKNOWLEDGMENTS: We acknowledge Nicholle Johnson, B.S., Howard Byrne, and Maribeth Stansifer, B.S., for their work. This study was supported in part by grants from the Department of Veterans Affairs, the WARMER Foundation, The Hansjörg Wyss Foundation, and the Biomedical Research and Education Foundation of Southern Arizona. Conflicts of interests: Theregen, Inc. provided the 3DFC patch but did not provide any financial support for these studies. The University of Arizona has a licensing agreement with Theregen to use the 3DFC patch in the heart. Drs. Thai, Kellar, and Goldman are consultants for Theregen and Dr. Williams is on the Advisory Board for Theregen.

REFERENCES

1. Assmus, B.; Honold, J.; Schachinger, V.; Britten, M. B.; Fischer-Rasaokat, U.; Lehmann, R.; Teupe, C.; Pistorius, K.; Martin, H.; Abolmaali, N. D.; Tonn, T.; Dimmeler, S.; Zeiher, A. Transcoronary transplantation of progenitor cells after myocardial infarction. N. Eng. J. Med. 355: 1222–1232; 2006.
2. Balsam, L. B.; Wagers, A. J.; Christensen, J. L.; Kofidis, T.; Weissman, I. L.; Robbins, R. C. Haematopoietic stem cells adopt mature haematopoietic fates in ischaemic myocardium. Nature 428:668–673; 2004.
3. Bodo, E. S.; Michael, B.; Tobias, Z.; Thomas, B.; Christina, S.; Christine, A.; Rüdiger, V. S.; Gesine, K.; Peter, W.; Hans-Wilhelm, M.; Matthias, K. Regeneration of human infarcted heart muscle by intracoronary autologous bone marrow cell transplantation in chronic coronary artery disease: The IACT study. J. Amer. Col. Cardiol. 46: 1651–1658; 2005.
4. Chachques, J. C.; Traninini, J.; Lago, N.; Masoli, O.; Barisani, J.; Cortes-Morichetti, M.; Schussler, O.; Carpentier, A. Myocardial assistance by grafting a new bioartificial

upgraded myocardium (MAGNUM Clinical Trial): One year follow-up. Cell Transplant. 16:927–934; 2007.
5. Cohen, S.; Leor, J. Rebuilding broken hearts. Sci. Am. 291:45–51; 2004.
6. Fujimoto, K. L.; Tobita, K.; Merryman, D.; Guan, J.; Momoi, N.; Stolz, D. B.; Sacks, M. S.; Keller, B. R.; Wagner, W. R. An elastic, biodegradable cardiac patch induces contractile smooth muscle and improves cardiac remodeling and function in subacute myocardial infarction. J. Amer. Col. Cardiol. 49:2292–2300; 2007.
7. Fukuda, S.; Kaga, S.; Sasaki, H.; Zhan, L.; Zhu, L.; Otani, H.; Kalfin, R.; Das, D. K.; Maulik, N. Angiogenic signal triggered by ischemic stress induces myocardial repair in rat during chronic infarction. J. Mol. Cell. Cardiol. 4:547–559; 2004.
8. Gaballa, M. A.; Goldman, S. Ventricular remodeling in heart failure. J. Cardiac Failure 6:S476–S485; 2002.
9. Gaballa, M. A.; Raya, T. E.; Goldman, S. Large artery remodeling after myocardial infarction. Am. J. Physiol. 268:H2092–H2103; 1995.
10. Gaballa, M. A.; Sunkomat, J. N. E.; Morkin, E.; Ewy, G.; Goldman, S. Grafting an acellular 3-D collagen scaffold onto a non-transmural cryoinjured myocardium induces neoangiogenesis and retards cardiac remodeling. J. Heart Lung Transplant. 25:946–954; 2006.
11. Gaudette, G. R.; Cohen, I. S. Cardiac regeneration material can improve the passive properties of myocardium, but cell therapy must do more. Circulation 114:2575–2577; 2006.
12. Goldman, S.; Raya, T. E. Rat infarct model of myocardial infarction and heart failure. J. Cardiac Failure 1:169–177; 1995.
13. Janssens, S.; Dubois, C.; Bogaert, J.; Theunissen, K.; Deroose, C.; Desmet, W.; Kalantzi, M.; Herbots, L.; Sinnaeve, P.; Dens, J.; Maertens, J.; Rademakers, F.; Dymarkowski, S.; Gheysens, O.; Van Cleemput, J.; Bormans, G.; Nuyts, J.; Belman, A.; Mortelmans, L.; Boogaerts, M.; Van de Werf, F. Autologous bone marrow-derived stem-cell transfer in patients with ST-segment elevation myocardial infarction; double blind, randomized controlled trial. Lancet 367:113–121; 2006.
14. Kajstura, J.; Rota, M.; Whang, B.; Cascapera, S.; Hosoda, T.; Bearzi, C.; Nurzynska, D.; Kasahara, H.; Zias, E.; Bonafé, M.; Nadal-Ginard, B.; Torella, D.; Nascimbene, A.; Quaini, F.; Urbanek, K.; Leri, A.; Anversa, P. Bone marrow cells differentiate in cardiac cell lineages after infarction independently of cell fusion. Circ. Res. 96:127–137; 2005.
15. Kellar, R. S.; Landeen, L. K.; Shepherd, B. R.; Naughton, G. K.; Ratcliffe, A.; Williams, S. K. Scaffold-based 3-D human fibroblast culture provides a structural matrix that support angiogenesis in infarcted heart tissue. Circulation 104:2063–2068; 2001.
16. Kellar, R. S.; Shepherd, B. R.; Larson, D. F.; Naughton, G. K.; Williams, S. K. A cardiac patch constructed from human fibroblasts attenuates a reduction in cardiac function following acute infarct. Tissue Eng. 11(11–12):1678–1687; 2005.
17. Kern, A.; Liu, K.; Mansbridge, J. Modification of fibroblast gamma-interferon responses by extracellular matrix. Invest. Dermatol. 17:112–118; 2001.
18. Lei, L.; Zhou, R.; Zheng, W.; Christensen, L.; Weiss, R.; Tomanek, R. Bradycardia induces angiogenesis, increases coronary reserve, and preserves function of the postinfarcted heart. Circulation 110(7):796–802; 2004.
19. Lunde, K.; Solheim, S.; Aakhus, S.; Arnesen, H.; Abdelnoor, M.; Egeland, T.; Endresen, K.; Ilebekk, A.; Mangschau, A.; Fjeld, J. G.; Smith, H. J.; Taraldsrud, E.; Grøgaard, H. K.; Bjørnerheim, R.; Brekke, M.; Müller, C.; Hopp, E.; Ragnarsson, A.; Brinchmann, J. E.; Forfang, K. Intracoronary injection of mononuclear bone marrow cells in acute myocardial infarction. N. Eng. J. Med. 355:1199–1209; 2006.
20. Mansour, S.; Vanderheyden, M.; De Bruyne, B.; Vandekerckhove, B.; Delrue, L.; Van Haute, I.; Heyndrickx, G.; Carlier, S.; Rodriguez-Granillo, G.; Wijns, W.; Bartunek, J. Intracoronary delivery of hematopoietic bone marrow stem cells and luminal loss of the infarct-related artery in patients with recent myocardial infarction. J. Am. Col. Cardiol. 47:1727–1730; 2006.
21. Murry, C. E.; Soonpaa, M. H.; Reinecke, H.; Nakajima, H.; Nakajima, H. O.; Rubart, M.; Kishore, B.; Pasumarthi, S.; Virag, J. I.; Barteimez, S. H.; Poppa, V.; Bradford, G.; Dowell, J. D.; Williams, D. A.; Filed, L. J. Haematopoietic stem cells do not transdifferentiate into cardiac myocytes in myocardial infarcts. Nature 428:664–668; 2004.
22. Oz, M. C.; Konertz, W. F.; Kleber, F. X.; Mohr, F. W.; Gummert, J. F.; Ostermeyer, J.; Lass, M.; Raman, J.; Acker, M. A.; Smedira, N. Global surgical experience with the Acron cardiac support devise. J. Thoracic Cardiovasc. Surg. 126:983–991; 2003.
23. Patel, A. N.; Sherman, W. Cardiac stem cell therapy from bench to bedside. Cell Transplant. 16:875–878; 2007.
24. Pennock, G. D.; Raya, T. E.; Bahl, J. J.; Goldman, S.; Morkin, E. Combination treatment with captopril and the thyroid hormone analog 3,5-diiodothyroproprionic acid (DITPA): A new approach to improving left ventricular performance in heart failure. Circulation 88:1289–1298; 1993.
25. Raya, T. E.; Gaballa, M.; Anderson, P.; Goldman, S. Left ventricular function and remodeling after myocardial infarction in aging rats. Am. J. Physiol. 273(6 Pt. 2):H2652–H2658; 1997.
26. Raya, T. E.; Gay, R. G.; Aguirre, M.; Goldman, S. The importance of venodilatation in the prevention of left ventricular dilatation after chronic large myocardial infarction in rats: A comparison of captopril and hydralazine. Circ. Res. 64:330–338; 1989.
27. Reinhardt, C. P.; Dalberg, S.; Tries, M. A.; Marcel, R.; Leppo, J. A. Stable labeled micorspheres to measure perfusion: validation of a neutron activation assay technique. Am. J. Physiol. 280:H108–H116; 2001.
28. Schächinger, V.; Assmus, B.; Britten, M. B.; Honold, J.; Lehmann, R.; Teupe, C.; Abolmaali, N. D.; Vogl, T. J.; Hofmann, W. K.; Martin, H.; Dimmeler, S.; Zeiher, A. M. Transplantation of progenitor cells and regeneration enhancement in acute myocardial infarction final one-year results of the TOPCARE-AMI Trial. J. Amer. Col. Cardiol. 44:1690–1699; 2004.
29. Schächinger, V.; Erbs, S.; Elsasser, A. Intracoronary bone marrow-derived progenitor cells in acute myocardial infarction: A randomized, double-blind, placebo controlled multicenter trial (REPAIR-AMI). N. Eng. J. Med. 355: 1210–1221; 2006.
30. Schächinger, V.; Erbs, S.; Elsässer, A.; Haberbosch, W.; Hambrecht, R.; Hölschermann, H.; Yu, J.; Corti, R.; Mathey, D. G.; Hamm, C. W.; Süselbeck, T.; Werner, N.; Haase, J.; Neuzner, J.; Germing, A.; Mark, B.; Assmus, B.; Tonn, T.; Dimmeler, S.; Zeiher, A. M.; REPAIR-AMI Investigators. Improved clinical outcome after intracoro-

nary administration of bone-marrow-derived progenitor cells in acute myocardial infarction: Final 1-year results of the REPAIR-AMI trial. Eur. Heart J. 27:2775–2783; 2006.
31. Schwartz, R. C. The politics and promise of stem-cell research. N. Eng. J. Med. 355:1189–1199; 2006.
32. Strauer, B. E.; Brehm, M.; Zeus, T.; Bartsch, T.; Schannwell, C.; Antke, C.; Sorg, R.; Kögler, G.; Wernet, P.; Müller, H.; Köstering, M. Regeneration of human infarcted heart muscle by intracoronary autologous bone marrow cell transplantation in chronic coronary artery disease. The IACT Study. J. Am. Col. Cardiol. 46:1651–1658; 2005.
33. Thai, H.; Castellano, L.; Juneman, E.; Phan, H.; Do, R.; Gaballa, M. A.; Goldman, S. Pretreatment with angiotensin receptor blockade prevents left ventricular dysfunction and blunts LV remodeling associated with acute myocardial infarction. Circulation 114:1933–1939; 2006.
34. Wagers, A. J.; Sherwood, R. I.; Christensen, J. L.; Weissman, I. L. Little evidence for developmental plasticity of adult hematopoietic stem cells. Science 297:2256–2259; 2002.
35. Wall, S. T.; Walker, J. C.; Healy, K.; Ratcliffe, M. B.; Guccione, J. Theoretical impact of the injection of material into the myocardium: A finite element model simulation. Circulation 114:2627–2635; 2006.
36. Wollert, K. C.; Meyer, G. P.; Lotz, J.; Lichtenberg, S.; Lippolt, P.; Breidenbach, C.; Fichtner, S.; Korte, T.; Hornig, B.; Messinger, D.; Arseniev, L.; Hertenstein, B.; Ganser, A.; Drexler, H. Intracoronary autologous bone-marrow cell transfer after myocardial infarction: The BOOST randomized controlled clinical trial. Lancet 364: 141–148; 2004.